Deformation Characteristics of Geomaterials
V.A. Rinaldi et al. (Eds.)
IOS Press, 2015

doi:10.3233/978-1-61499-601-9-850

Inherent Anisotropy of an Undisturbed and Compacted Loess Soil

Pedro A. COVASSI[a,1] and Victor A. RINALDI[a]
[a] *Facultad de Ciencias Exactas, Físicas y Naturales. Universidad Nacional de Córdoba*

Abstract. This work discusses the result of an experimental study on inherent anisotropy of the loess soil found at Córdoba, Argentina. A cubical true triaxial device provided with flexible boundaries was used and the samples were subjected to an isotropic compression stress path. A brief description of the true triaxial device as well as the procedure for its assemblage and testing procedure is presented. Tests were performed on undisturbed and compacted samples. Undisturbed block type samples were recovered from open trenches. Compacted samples were made either by tamping or static compaction. The effect of compaction method on structural anisotropy was evaluated. Samples were prepared at dry of optimum, optimum and wet of optimum. Isotropic compression tests show that inherent structural anisotropy is found in both undisturbed and compacted specimens. Undisturbed samples are less compressible and develop higher degree of strain anisotropy respect the compacted samples at the same dry unit weight.

Keywords. Inherent Anisotropy, Loess, True Triaxial Test, Compaction method.

1. Introduction

Argentinean loess in one of the largest deposits on the world, with thickness varying between 25 and 60 m ([1], [2], [3], [4]). Loess is an eolian low dense formation (usually densities range between 11.5 kN/m^3 and 13.5 kN/m^3) composed by fine sand and silt particles and a minor clay fraction (mainly illite and montmorillonite) weakly bonded. Under natural conditions, loess is able to withstand vertical slopes and to sustain moderate stresses without significant deformations. In this state, both stiffness and strength of this soil is governed by matric suction and cementation provided by precipitated salts at particle contacts. Upon saturation, soluble salts dissolve, capillary forces decrease, the structure weakens and collapse takes place, sometimes under self-weight of the soil. Actually, it is difficult to differentiate the individual role of cementation and suction in the collapse process [3].

Due to the large extent of loess deposits of Argentina, this soil is used in most earthworks including excavations, tunneling, liners for waste and wastewater containment, embankments, backfills, core dams, and hydraulic barriers. Improvement of mechanical behavior of loess is usually achieved by means of static and dynamic compaction in the field. The compaction procedure destroys cemented bonds and consequently the collapse potential is significantly reduced [3].

At present, there are several research works on Argentinean loess mainly focused in understanding the collapse mechanism, the relationship between collapse and soil structure, the stress-strain behavior in situ and laboratory, and the behavior of maximum shear modulus (G_{max}) ([5], [6], [7], [8], [9], [10]). Limited research has been

[1] Corresponding Author.

done for saturated undisturbed samples in drained conditions using the conventional triaxial test device [11], [12].

This work presents an experimental study performed to evaluate the inherent anisotropic behavior on undisturbed and compacted loess samples. A series of isotropic compression tests over natural undisturbed and compacted samples were done in a flexible boundaries cubical true triaxial device.

2. Soil Description and Testing Program

The soil used here includes both undisturbed and compacted loessial samples obtained from the loess formation in Córdoba city, Argentina. Undisturbed block samples were retrieved from a vertical wall at approximately 6 m depth of an open trench located at a highway construction project in the North-West of Córdoba City. The samples were placed in plastic bags and stored in a conditioned room for preservation of initial water content and temperature. An average dry unit weight of $\gamma_d = 13.4$ kN/m^3 for undisturbed specimens was measured. Natural moisture content of undisturbed samples was around $w_{nat} = 12.5$ %. Compacted samples were made from air dried soil, sieved through sieve No. 40 (425 μm) and mixed thoroughly. The standard Proctor test yielded a maximum dry unit weight of $\gamma_d = 16{,}3$ kN/m^3 at the optimum moisture content of $w_{opt} = 18{,}7$ %. Other relevant physical properties of the soils tested are summarized in Table 1.

Table 1. Physical properties and classification of soils tested.

Soil	PL [%]	LL [%]	PI [%]	Gs	Passing Sieve #40 [%< 425 μm]	Passing Sieve #60 [%< 250 μm]	Passing Sieve #200 [%< 74 μm]	Clay Content [% < 2 μm]	SC
Compacted	18.8	24.3	5.5	2.67	100	92.2	81.3	15.1	ML
Natural	NP	21.7	NP	2,66	100	98.5	90.3	9.6	ML

Note: PL: Plastic Limit; LL: Liquid Limit; PI: Plasticity Index; Gs: Specific Gravity; SC: Unified Soil Classification; NP: Nonplastic.

Compacted specimens were prepared by two compaction methods: dynamic and static. The soil used for compacted specimens was mixed with the desired amount of water, placed in a hermetic recipient and allowed to reach equilibrium for 24 hr. Each specimen was compacted in four layers of approximately the same height [13]. The dynamically compacted specimen was prepared by wet tamping in a two-piece split cubical steel mold of 80 mm in side dimension. Compaction energy of 1.51 kg.cm/cm^3 (corresponding to a quarter of the energy of Standard Proctor Test, ASTM D 698) was applied and the moisture content of 16.4% (dry side of the Standard Proctor curve) was selected. Figure 1 shows the Standard Proctor curve for the tested soil and the initial density and water content conditions of prepared specimens. Static compacted specimens were prepared in a two-piece split cubical acrylic mold of 80 mm in side dimension using the compaction procedure described by Cui and Delage [14]. Compaction was performed in four layers at a compression rate of 1 mm/min in a triaxial loading frame until the average value of $\gamma_d = 13.4$ kN/m^3 was obtained for all the compacted samples and at three different moisture contents (see Figure 2). Table 2

summarizes the initial conditions of the different soil specimens prepared and tested in the present work.

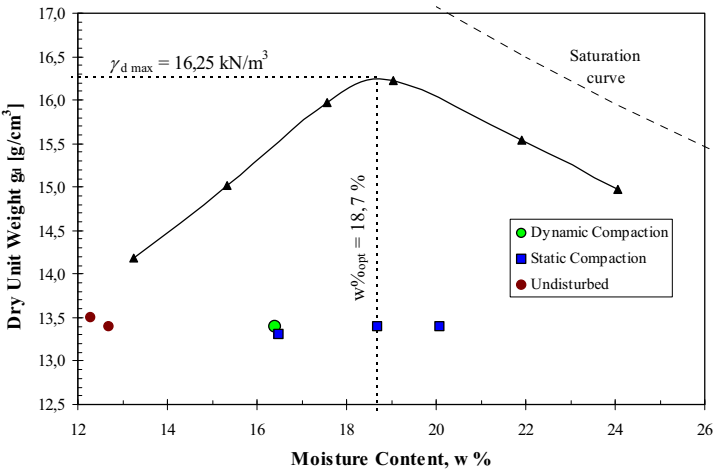

Figure 1. Compaction moisture content and dry unit weight of the different specimens prepared.

Table 2. Initial state conditions for the different specimens tested in this work.

Group	Sample Designation	γ_d [kN/m^3]	$w_{comp/nat}$ [%]	Max. Stress Level Measured in Static Compaction [kPa]
Dynamic Compaction	D-D (Dry of optimum)	13.4	16.4	-
Static Compaction	S-D (Dry of optimum)	13.3	16.5	74
	S-O (optimum)	13.4	18.7	40
	S-W (Wet of optimum)	13.4	20.1	24
Undisturbed Loess	S1	13.5	12.3	-
	S2	13.4	12.7	-

A flexible boundaries type cubical true triaxial apparatus developed in the Geotechnical Laboratory of National University of Córdoba was used for testing. The design was based on similar devices described elsewhere ([15], [16] [17]). Figure 2 sketches the cubical cell and peripherals. The cubical triaxial apparatus allows for the application of three mutually and independently perpendicular principal stresses. In this device, the aluminum reaction frame holds an 80 mm cubical specimen. Drainage, vacuum, and pore water pressure monitoring ports were drilled diagonally as shown on the same Figure 2. Each side wall assembly contains a linear variable deformation transducer (LVDT) for measuring deformations at the center of each face of the specimen and a ¼ in. hole to apply the air pressure. Three of the wall assemblies also provide ½ in. outlets to connect a pressure transducer. All electronic transducers are connected to a computer. A specific software was developed for tests control and data storage. A Tri-Flex 2 Master Control Panel (ELE International) is connected to the drainage ports for pressure control and saturation of the specimens.

The use of flexible membranes allows boundary stresses to be uniform over the faces of a specimen. In this work, the non-uniform distribution of deformations at each

sample face was evaluated using a simple profilometer [16] and a high density expanded polystyrene cubical specimen to check the displacements contours experienced under isotropic compression at two stress levels, 50 and 100 kPa. The results of this calibration allows to conclude that the displacements contours are reasonably uniform at relative large strains and that the displacement values obtained in the center point of the membrane using LVDTs are reliable and representative in a similar fashion as obtained by other authors [16], [18], [19]. Strain corrections related to membrane compression were incorporated in strain computations, although they were found to be very small respect to the strain levels measured in this work.

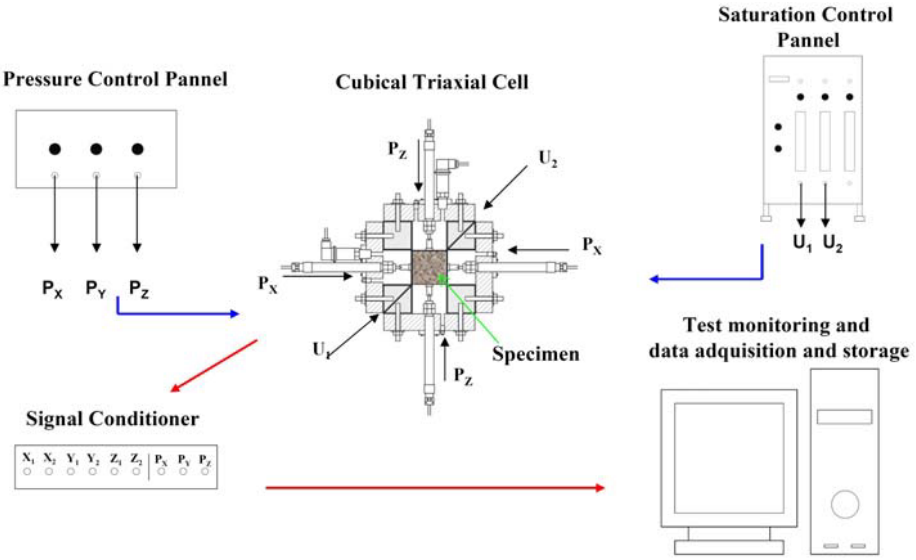

Figure 2. Test setup of the Cubical True Triaxial Device used in this work.

The prepared specimens were installed in the cubical triaxial cell, and all the parts of the true triaxial device were assembled. Then, the specimens were permeated for 24 hours with de-aired water from the lower drainage port. Saturation of the specimen was increased using back pressure until de pore pressure parameter B was above 0.90 at the applied back pressures of 100 kPa. After saturation, samples were tested under an isotropic drained compression stress path. Initial effective stress level for all tests was set at 20 kPa with stress increments of 20 kPa up to 100 kPa. After this value was reached, stress increments were of 50 kPa. Each stress increment was maintained until primary consolidation ended which, for most samples, took place after 30 min.

3. Experimental Results and Discussions

Figure 3 shows the measured isotropic compressibility curves for the principal directions (x, y and z) for the two undisturbed loess specimens tested. Here, z direction (ε_Z) is always perpendicular to the bedding plane and coincident with respect the in-situ vertical direction, while the strains reported in x and y directions (ε_X and ε_Y) are parallel to the bedding plane and coincident with the in-situ horizontal directions.

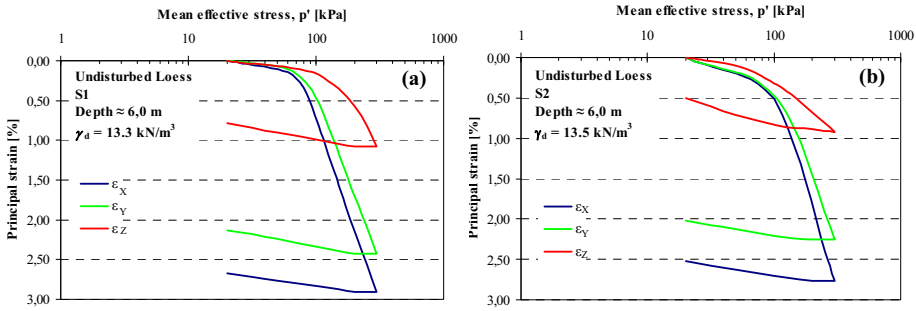

Figure 3. Compressibility curves of two undisturbed samples of loess under isotropic test conditions.

Results of Figure 3 show that compressibility of loess is higher in the horizontal directions respect to the vertical direction. Similarly, yielding is clearly observed in all curves being yielding pressure in vertical direction much higher than that in the horizontal directions. Also small differences are observed between the horizontal compressibility curves. Although the differences between compressibility curves in the horizontal direction are small, such differences exists and it may be possibly attributed either to: a) the in-situ state of stress conditions experienced by the soil in the face of the open trench after excavation (the *y* direction is parallel to the face of the trench) or b) to the deposition direction of the disk shape silt particles which main axis is usually oriented to S-N direction in coincidence with the dominant deposition winds at the site.

Figure 4 shows the measured isotropic compressibility curves in the principal directions (*x*, *y* and *z*) for dynamic and static compacted specimens at similar initial water content (dry of optimum) and unit weight. Here, compressibility is much higher than that corresponding to the undisturbed specimens at the same dry unit weight and moisture content. Additionally, compressibility in the horizontal directions *x* and *y* are quite similar and higher than that corresponding to the vertical direction. The results in this case clearly show that the behavior of compacted specimens is cross-anisotropic with stiffer response in the vertical direction. Observe that yielding is not well defined or may be very low in all cases.

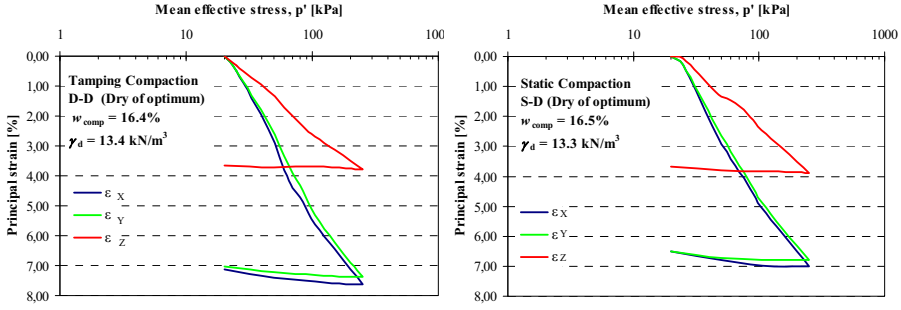

Figure 4. Compressibility curves of two compacted specimens under isotropic compressions stress path: **(a)** tamping compaction (dynamic); **(b)** Static compaction.

The deformation anisotropy can also be evaluated by comparing the strains in different directions. The difference between strains on each direction was determined

using the average relative difference (*ARD*) [20], which for the *x* direction can be written as:

$$ARD[\%] = \left\{ \frac{1}{n} \sum_{i=1}^{i=n} \frac{\left| \varepsilon_{x,i} - \varepsilon_{av,i} \right|}{\varepsilon_{x,i}} \right\} 100 \quad (1)$$

Where n is the number of stress loading steps, $\varepsilon_{x,i}$ is the strain in a specific direction (x in this case) for a specific stress level n = i, and $\varepsilon_{av,i}$ is the average strain for the same stress level i. Alternating the x index by y and z, *ARD* values for the other two directions could be calculated. Notice that *ARD* varies between 0% for isotropic behavior and any positive value for an anisotropic response. The higher the *ARD* value the higher the anisotropy. The values of *ARD* calculated respect to the three directions for all the tests performed in this work are displayed on Table 3 being the z direction coincident with the vertical direction. From the results of Table 3, it is observed that the higher ARD values are obtained respect to z directions while the values in the x and y directions being similar and much lower than for the z direction. The highest ARD corresponds to the undisturbed specimens. Also, undisturbed specimens of loess show similar behavior.

Table 3. Summary of different specimens tested in this work.

Group	Sample Designation	*Comparison between strains*	*ARD [%]*
Dynamic Compaction	D-D (Dry of optimum)	ε_X to the mean*	18
		ε_Y to the mean*	14
		ε_Z to the mean*	65
Static Compaction	S-D (Dry of optimum)	ε_X to the mean*	18
		ε_Y to the mean*	15
		ε_Z to the mean*	71
	S-O (optimum)	ε_X to the mean*	15
		ε_Y to the mean*	25
		ε_Z to the mean*	46
	S-W (Wet of optimum)	ε_X to the mean*	10
		ε_Y to the mean*	15
		ε_Z to the mean*	68
Undisturbed Loess	S1	ε_X to the mean*	28
		ε_Y to the mean*	11
		ε_Z to the mean*	106
	S2	ε_X to the mean*	25
		ε_Y to the mean*	12
		ε_Z to the mean*	105

Note: * mean = $(\varepsilon_X + \varepsilon_Y + \varepsilon_Z)/3$

Lade and Abelev [21] used the angle of inclination of the total strain increment vector to the hydrostatic axis (θ) to characterize the anisotropic behavior under an isotropic compression stress path, which is defined as:

$$\tan\theta = \frac{\sqrt{2}}{2}(1 - 3\rho) \quad (2)$$

Where $\rho = d\varepsilon_z/d\varepsilon_{vol}$ for total strain increments. The angle θ is considered positive when the strain increment is pointing downwards from hydrostatic axis. This corresponds to the case for cross-anisotropic soil deposits that are stiffer in vertical direction. A value of zero in θ corresponds to an isotropic material. The increasing mean confining pressure tends to override the effect of anisotropy.

Figure 5 shows the variation of θ with confining effective stress for all test performed on compacted specimens in this work. Curves that best approximate the experiments for each test are also included (dashed lines). Results show decreasing values of θ with increasing isotropic effective pressure. Also, for the pressure range used in this work, no specimen developed isotropic behavior.

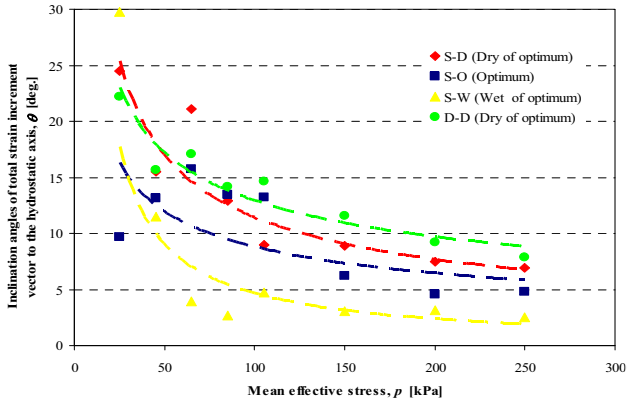

Figure 5. Variations of inclination angle θ with mean confining pressure for compacted specimens.

4. Conclusions

Inherent anisotropy of natural and compacted loess soil under an isotropic compression stress path have been evaluated. Results of isotropic compression tests show that compacted loess soil behaves as a cross-anisotropic material, presenting a higher stiffness in vertical direction. Anisotropy was also analyzed by means of the relative difference (*ARD*) of principal strains and the inclination angle of total strain increment vector (θ). These approaches showed that anisotropy seems to be unaffected by the two compaction methods and sample moisture. Undisturbed loess specimens seem to behave as orthotropic materials. However, differences between the horizontal strains are much smaller than the difference between the vertical and the average horizontal strains.

References

[1] R.J. Rocca, Review of Properties of Loess Soils, CE 299 Report presented at the University of California, Berkeley, CA, 1985.

[2] L. Moll and R.J. Rocca, Properties of Loess in the Center of Argentina, Proceedings of the IX Panamerican Conference on Soil Mechanics and Foundation Engineering, Chile (1991), Vol. 1, 1-13.

[3] V.A. Rinaldi, J.J. Clariá and J.C. Santamarina, The Small-strain Shear Modulus (G_{max}) of Argentinean Loess, Proceedings of the 15 International Conference on Soil Mechanics and Geotechnical Engineering, Istambul, Turkey (2001), 495-499.
[4] R.J. Rocca, E.R. Redolfi and R.E. Terzariol, Geotechnical Characteristics of Argentinean Loess, Rev. Int. de Desastres Naturales, Accidentes e Infraestructura Civil, Vol. 6 (2) (2006), 149-166. (In Spanish).
[5] A. Reginatto, Standard Penetration Test in Collapsible Soils, Proceedings of the IV Panamerican Conference on Soil Mechanics and Foundation Engineering, Puerto Rico, (1971), Vol. II, 77-84.
[6] V.A. Rinaldi, J.C. Santamarina and E.R. Redolfi, Characterization of Collapsible Soils With Combined Geophysical and Penetration Testing. Symposium In-Situ Characterization of Soils, Atlanta USA (1998). Vol. 1, 581-588.
[7] V.A. Rinaldi and J.J. Clariá, Low Strain Dynamic Behavior of a Collapsible Soil, Proceedings of the XI Panamerican Conference on Soil Mechanics and Foundation Engineering, Foz de Iguazu, Brazil (1999), Vol. 2, 835 – 841.
[8] V.A. Rinaldi and J.A. Capdevila, Effect of Cement and Saturation on the Stress Strain Behavior of a Silty Clay. Proceedings of Fourth International on Unsaturated Soils, G.A. Miller, C.E. Zapata, S.L. Houston, and D.G. Fredlund eds. ASCE (2006), VA, Vol 2, 1157-1168.
[9] F.M. Francisca, Evaluating the Constrained Modulus and Collapsibility of Loess from Standard Penetration Test, International Journal of Geomechanics (2007), 7(4), 307-310.
[10] V.A. Rinaldi, R.J. Rocca and M.E. Zeballos, Geotechnical Characterization and Behavior of Argentinean Collapsible Loess, on: Characterization and Engineering Properties of Natural Soils, Tan T. S. *et al.* eds. (2007), Balkema, London, Vol. 4, 2259-2286.
[11] J.A. Capdevila, *Personal communication*, 2014.
[12] J.A. Capdevila and V.A. Rinaldi, Local and Global Measurement of Strains in Triaxial Cell: Influence of Soil Conditions, Proceedings of the XIII Panamerican Conference on Soil Mechanics and Foundation Engineering, Isla Margarita, Venezuela (2007).
[13] V. Sivakumar and S.J. Wheeler, Influence of compaction procedure on the mechanical behaviour of an unsaturated compacted clay. Part 1: Wetting and isotropic compression, Géotechnique **50** (2000), No. 4, 359–368.
[14] Y.J. Cui and P. Delage, Yielding and Plastic Behaviour of an Unsaturated Compacted Silt, Géotechnique **46** (1996), No. 2, 291-311.
[15] J.H. Park, Performance and Check-out Verification Testing of a New True Triaxial Apparatus using Partially Saturated Silty Sand, M. Sc. Thesis The University of Texas at Arlington (2005).
[16] C.H. Choi, P. Arduino and M.D. Harney, Development of a True Triaxial Apparatus for Sands and Gravels, Geotechnical Tesing Journal, Vol. 31, No. 1, 2008, 1 – 13.
[17] L.R. Hoyos, D.D. Pérez-Ruiz and A.J. Puppala, A refined True Triaxial Apparatus for Testing Unsaturated Soils under Suction-controlled Stress Paths, International Journal of Geomechanics, Vol. 12, No. 3, (2012), 281-291.
[18] D. Mandeville and D. Penumadu, True Triaxial System for Clay with Proportional-Integral-Differential (PID) Control, Geotechnical Tesing Journal, Vol. 27, No. 2, 2004, 1 – 11.
[19] A. Prashant and D. Penumadu, Effect of Intermediate Principal Stress on Overconsolidated Kaolin Clay, Journal of Geotechnical and Geoenvironmental Engineering, Vol. 130, No. 3, (2004), 284-292.
[20] F. Li and V.M. Puri, Measurement of anisotropic behavior of dry cohesive and cohesionless powders using a cubical triaxial tester, Powder Technology **89** (1996), 197-207.
[21] P.V. Lade and A.V. Abelev, Characterization of cross-anisotropic soil deposits from isotropic compression tests, Soils and Foundations **45** (2005), No. 5, 89-102.